Taylor & Francis
Taylor & Francis Group

Journal of Dispersion Science and Technology

ISSN: 0193-2691 (Print) 1532-2351 (Online) Journal homepage: https://www.tandfonline.com/loi/ldis20

Development of polylactic acid (PLA) bio-composite films reinforced with bacterial cellulose nanocrystals (BCNC) without any surface modification

Endarto Y. Wardhono, Nufus Kanani, Alfirano & Rahmayetty

To cite this article: Endarto Y. Wardhono, Nufus Kanani, Alfirano & Rahmayetty (2019): Development of polylactic acid (PLA) bio-composite films reinforced with bacterial cellulose nanocrystals (BCNC) without any surface modification, Journal of Dispersion Science and Technology, DOI: 10.1080/01932691.2019.1626739

To link to this article: https://doi.org/10.1080/01932691.2019.1626739

JOURNAL OF DISPERSION SCIENCE AND TECHNOLOGY
https://doi.org/10.1080/01932691.2019.1626739

Development of polylactic acid (PLA) bio-composite films reinforced with bacterial cellulose nanocrystals (BCNC) without any surface modification

Endarto Y. Wardhono, Nufus Kanani, Alfirano, and Rahmayetty

Engineering Faculty, University of Sultan Ageng Tirtayasa, Cilegon, Indonesia

ABSTRACT

In this work, polylactic acid (PLA) matrix was reinforced with bacterial cellulose nanocrystals (BCNC) to form bio-composite films. The films were produced via two step processes; (1) isolation of BCNC from commercial nata de coco (bacterial cellulose) under catalytic hydrolysis using metal chloride salt (FeCl3.6H2O) assisted by ultrasonic irradiation; (2) fabrication of PLA/BCNC bio-composite films by a solvent casting method. The effect of BCNC incorporation into bio-composite by addition at different concentrations (2.5%, 5%, 7.5% and 10% w/w of BCNC) was evaluated on the chemical structure, crystallinity, thermal properties, morphology and mechanical properties without any surface modification of reinforcement material previously. The results demonstrated that cellulose nanocrystal from bacterial cellulose can improve the mechanical properties of PLA-based biomaterial film. The developed PLA/BCNC bio-composites films can potentially be used for edible packaging materials.

GRAPHICAL ABSTRACT

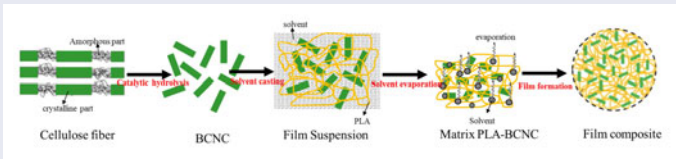

ARTICLE HISTORY
Received 29 January 2019
Accepted 24 May 2019

KEYWORDS
Word; PLA; ultrasonic irradiation; BCNC; bio-composite films; solvent casting

Introduction

Poly (lactic) acid (PLA) is linear aliphatic thermoplastic polyester which derived by chemical conversion of corn starch or other sugar feed stocks into lactic acid then followed by ring opening polymerization of lactide monomer thus forming long chain molecular compounds.[1,2] PLA is a green alternative material to replace the use of petroleum-based plastic film which known as the main source of post-consumer waste leading to pollution today. The most advantageous characteristic of PLA is renewability, biocompatibility and inherent biodegradability.

The most important characteristics of packaging films is rigid and flexible that makes them very durable. PLA by nature is a brittle polymer with less than 10% of elongation at break.[3,4] It also has limited gas barrier capacity due to its hydrophobic character. Despite its strong resistance (tensile strength from 17 to 74 MPa),[5,6] PLA is a semi crystalline polymer and consequently has low heat resistance (low modulus at high temperature) and low ductility and toughness,[7] however, have hindered PLA to be widely used as food packaging applications. A way to improve the properties of PLA and greatly enhance their commercial potential is to incorporate with cellulose nanocrystals (CNC). Several studies have been reported the use of CNC as reinforcing material to the hydrophobic polymers.[8–17]

CNC is naturally synthesized compound which mainly obtained from plant cell walls. It is rod-like nanoparticles obtained by removing the amorphous regions while keeping the crystalline regions through acid hydrolysis of cellulose fibers.[18] Apart from plants, certain bacteria and algae are also known to produce cellulose in substantial quantities in a relatively pure form.[19] Bacterial cellulose (BC), for example, can be easily processed into microfibrils, nanofibrils and nanocrystals through a top-down approach. The most commonly employed method for producing bacterial cellulose nanocrystals (BCNC) of 10–50 nm diameter and 100–300 nm length is by subjecting native BC to acid solution hydrolysis in combination with ultrasonication.[18] Compare to plant cellulose, nanocrystals from BC displays high crystallinity, high modulus and strength are also found to impart superior properties to polymer composites.[20]

Chemical modification of CNC which is hydrophilic in nature was performed to make desirable changes on the surface to widen its application. The main challenge in

CONTACT Endarto Y. Wardhono endarto.wardhono@untirta.ac.id Engineering Faculty, University of Sultan Ageng Tirtayasa, Cilegon, Indonesia; Rahmayettiy rahmayetty@untirta.ac.id Engineering Faculty, University of Sultan Ageng Tirtayasa, Cilegon, Indonesia.
Color versions of one or more of the figures in the article can be found online at www.tandfonline.com/ldis.

achieving excellent performance of biocomposite PLA/CNC lies in attaining a homogeneous dispersion and a good interaction of CNC within the PLA matrix in particular without surface modifications of the CNC. A non-homogeneous dispersion decreases the final mechanical properties of the biocomposite produced. Concerning to the brittleness of PLA, the addition of plasticizers is a possible solution increase its flexibility.[21] Plasticizers act as a lubricant for the molecules allowing them to be more flexible and to eliminate the brittle characteristics of some polymers.

From those basis above, the objective of this work is to evaluate the effect of BCNC incorporation on the chemical structure, crystallinity, thermal properties, morphology and mechanical properties of PLA as biodegradable films. Native BC was used as a fiber source to produce BCNC due to its high purity, which excludes the need of carrying out the delignification for lignocellulosic materials. The PLA/BCNC biocomposite films are produced via two step processes; (1) isolation of BCNC from commercial nata de coco (bacterial cellulose) under catalytic hydrolysis assisted by ultrasonic irradiation; (2) fabrication of the biocomposite films by a solvent casting method

Materials and methods

Materials

Native bacterial cellulose is dried nata de coco pellicles, collected by Chimultiguna (Indramayu, Indonesia). Sodium hydroxide (NaOH), ethanol (C_2H_5OH), and hydrochloric acid (HCl) were purchased from Thermo Fischer Scientific. Metal chloride, $FeCl_3.6H_2O$, was purchased from Merck Indonesia. PLA with specific gravity of 1.24 g/cm^3 was supplied by Huaian Ruanke Trade, China. All the reagents and chemicals are used as a laboratory grade without further purification. Demineralized water (conductivity of 0.06 mScm^{-1}) produced by a purification chain was used for all experiments.

Methods

Pretreatment of BC

BC pellicles were maintained in 0.5% NaOH (w/v) at room temperature for 24 h, followed by rinsing in the drained water until a neutral pH attained and any chemicals used in the BC production removed. The cellulose was then sun dried for two days, powdered and sieved through 149 μm sieve (100 Mesh).

Isolation of BCNC

The isolation BCNC was conducted into two step processes:

- Disintegration of BC pellicles was prepared based on the work[22] which carried out using an ultrasonic processor (Vibra Cell, Type 72434, 100 Watts, horn diameter: 1.0 mm, Fisher Scientific, France). One gram (1% w/v) of BC powder was introduced into a 200-mL flat-bottom flask with a mixture of water/ethanol (50% w/w). The ultrasonic horn was placed at the center of the suspension, while the temperature was maintained at room temperature with a circulating water condenser. The suspension was constantly stirred at 300 rpm using magnetic stirring bar. The irradiation was carried out at constant f = 20 kHz for 120 min. The degraded product was immediately washed with water and filtered with Whatman filter paper no. 1 until the filtrate was neutral, then oven dried at 70 °C for 24 h.
- Catalytic hydrolysis of degraded BC sample (oven dry 0.5 g) was put into 150 mL water of 2.5 mol/L HCl and 5% w/v of $FeCl_3.6H_2O$. The flask was heated to 70 °C in the water bath sonicator (Q-Sonica USA, model Q55, 120 Watts) for 90 minutes. During the protocol, the suspension was stirred with a magnetic stirring bar at 200 rpm. Upon completion of the hydrolysis, the flask was removed from the water bath and cooled at ambient temperature. The hydrolyzed product was immediately washed with deionized water and transferred to a 50 mL plastic centrifuge tube and centrifuged at 12,000 rpm for 5 min (Jouan, MR 1812 Refrigerated Centrifuge, MN, USA) to remove residual acid and chemicals. The precipitate was purified by five washing cycles with deionized water followed by centrifugation at 12,000 rpm for 5 min then oven dried at 70 °C for 24 h.

Fabrication of biocomposite films

PLA/BCNC biocomposite films were prepared using a solvent casting method. 5% w/v of PLA was dissolved into 100 ml of chloroform and gently stirred (200 rpm) for overnight using magnetic stirrer at room temperature (25 °C). 1% w/v of BCNC powder was suspended into 100 ml of chloroform under vigorous stirring (500 rpm) for 8 h using a magnetic stirrer at room temperature. The PLA/BCNC biocomposites were then prepared by mixing of materials using a rotor stator homogenizer type Polytron-3100D (Kinematica AG, Switzerland) at room temperature. The rotor speeds were set up initially at 3000 rpm. 5 mL of BCNC solution was introduced drop by drop into 25 mL of the PLA solution using a syringe pipette for 5 minutes. The rotor speed was then increased gradually (1000 rpm per 30 seconds) up to 14,000 rpm. Agitation was kept at this speed for 15 minutes. Finally, the rate was decreased gradually within 30 seconds until the rotor system stopped then followed by sonication for 30 min at room temperature using a ultrasonic processor (Vibra Cell, Type 72434, Fisher Scientific, France). The mixture was then poured into greased glass molds, followed by drying at room temperature for 24 h. Subsequently, the prepared film was removed from the casting surface, then further dried at 60 °C in a vacuum dryer to remove the remaining chloroform to prevent its plasticizing effect.

Characterizations

Fourier transform infrared, FT-IR

FTIR study was performed by a Nicolet iS5 spectrometer (Thermo Scientific, USA) to determine the functional groups

present in the cellulose. The measurements were taking 32 scans for each sample with a resolution of 4 cm^{-1}, ranging from 400 cm^{-1} to 4000 cm^{-1} and scanning speed of 20 mm/sat.

X-ray diffraction, XRD

The crystallinity index (CrI) of the celluloses was investigated by XRD analysis. The measurements were performed in a D8 Advance (Bruker, USA). Samples were examined with a scanning angle of 2θ from 10° to 40° at a rate of 1°/min with the CuKα filtered radiation. The crystallinity was calculated using deconvolution method,[23] in which the diffraction profile was fitted by Gaussian function to find the contribution of each individual peak relative to the crystallographic planes and the amorphous background. The CrI was calculated according to equation 1 as follows;

$$\mathrm{CrI} = \left(\frac{A_{cr}}{A_{cr} + A_{am}}\right) \times 100\% \quad (1)$$

Where, A_{am} is the amorphous area, and A_{cr} is the sum of the area of the 101, 10$\bar{i}$, 002, 040 peaks.

Differential scanning calorimetry, DSC

The thermal behavior of the cellulose was performed by DSC. The samples were characterized on a DSC Q100 (TA Instruments, USA) under constant nitrogen flow (50 mL/min), from 25 to 400 °C, at a heating rate of 10 °C/min.

Scanning electron microscopy, SEM

The morphology of biocomposite film was measured by using the high-resolution JEOL-2100F TEM (Jeol, Japan). Samples were conventionally deposited on carbon coated copper grids. The size and diameter distribution particle were measured by image J (version 1.41 h) and origin pro-8 software

Mechanical properties

A tensile test machine (Strograph, Toyoseiki, Japan) was used to study the mechanical properties of the film specimens in general accordance with ASTM D882-02. The initial grip separation was set at 100 mm and cross-head speed at 50 mm/min. Tensile strength (TS) was calculated by dividing the maximum load on the film before failure by the cross-sectional area of the initial specimen. Elongation at break (Eb) was defined as the percentage change in the length of the specimen compared to the original length between the grips. At least five replicates for each type of film were tested.

Results and discussions

Chemical structure

FTIR spectroscopy was used to investigate changes in the chemical structure of the materials before and after treatment. During isolation of BCNC step, the spectra of BC as a raw material, degraded cellulose (D-BC) as a product of disintegration, and the isolated BCNC of catalytic hydrolysis are shown in Figure 1a.

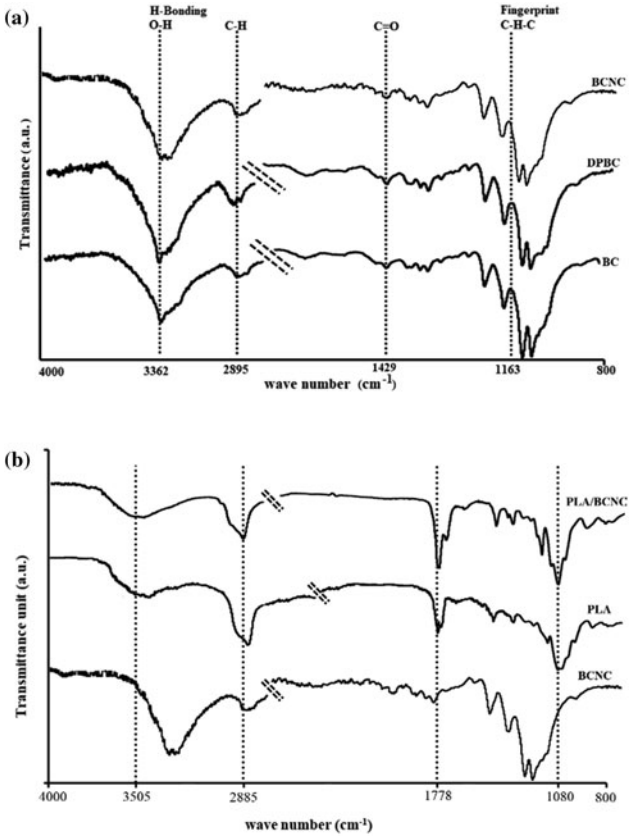

Figure 1. FTIR spectra of: (a) isolation of BCNC step (BC; D-BC; BCNC); (b) fabrication of biocomposite step (PLA; PLA/BCNC-5%).

FTIR analysis demonstrated that the chemical structures of all sample celluloses remained unchanged during both processes, ultrasonic irradiation and catalytic hydrolysis. The FTIR spectra displayed that the intensity of absorption of the functional groups between 4000 and 400 cm^{-1}. The spectra were divided into two parts: (1) H-bonding region from 4000 to 2600 cm^{-1}, and (2) fingerprint region from 1800 to 400 cm^{-1}.[24] The broad peak in the 3650-3000 cm^{-1} bands was assigned to O–H stretching vibrations, which are characteristic of the hydroxyl groups generally present in cellulose, water, and lignin. In this region, intra molecular hydrogen bonds appeared at 3342 cm^{-1} and 3432 cm^{-1}, and were attributed respectively to the two crystalline cellulose allomorphs, cellulose Iα and cellulose Iβ.[25] These hydroxyl groups were responsible for the stiffness in the polymer chain, and for allowing the linear polymers to form sheet structures.[26] The strong vibration band around 2895 cm^{-1} corresponded to C–H stretching vibrations.[27] This band may be associated with a hydrocarbonate linear chain. Higher values in this specific band are correlated to a decrease in the calculated total crystallinity value.[28] An intense band at 1429 cm^{-1} band can be assigned to the bending of asymmetric angular deformation of C-H bonds. The band found between 1420 to 1430 cm^{-1} was associated with the amount of the cellulose ordered form, while the band appearing at 898 cm^{-1} was assigned to the disordered

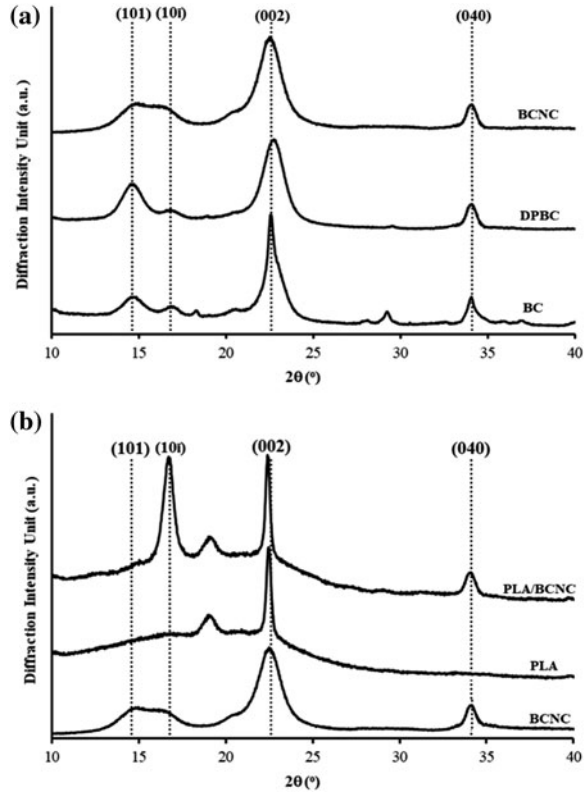

Figure 2. XRD pattern of: (a) isolation of BCNC step (BC; D-BC; BCNC); (b) fabrication of biocomposite step (PLA; PLA/BCNC-5%).

region.[29] The 1163 cm^{-1} band was assigned to asymmetrical stretching of C–O–C glycoside bonds.

The interactions of BCNC and PLA in the fabrication biocomposite films are presented in Figure 1b. The spectra of pure PLA displayed characteristic bands at 1778 cm^{-1} and 1080 cm^{-1}, which are attributed to the backbone ester group of PLA.[30,31] The -C-O- stretching vibration from the ester units was observed at 1080 cm^{-1}. The peak at 3505 cm^{-1} indicates the terminal -OH of L-lactic acid. The bands at 2885 cm^{-1} were assigned to the -C-H asymmetric and symmetric vibration of -CH_3 groups in the side chains. The band at 2945 cm^{-1} was attributed to the –CH- groups in the main chain of PLA. From the spectra of biocomposites film (PLA/BCNC-5% w/w), the bands around at 2885 and 980 cm^{-1} corresponding to –CH stretching and vibrations of –C–OH side groups. From the figure can be observed that the peaks at 2830, 2930, 3210 and 3300 cm^{-1}, which represents the hydroxyl functional groups) in the mixture PLA and BCNC. The peak at around 3010 cm^{-1} corresponds to the stretching vibration of the hydrogen bonded -OH groups. These indicate the presence of strong hydrogen bonded interaction between the PLA and the BCNC. In Figure 1b also shows the presence of the free C = O groups which correspond to the peak situated around 1778 cm^{-1}.[32]

Crystallinity index

The crystallinity index (CrI) of the samples was calculated by deconvolution methods, at which the diffraction profile was fitted by Gaussian function to find the contribution of each individual peak relative to the crystallographic planes and the amorphous background.[33,34] The XRD patterns of the sample BC, D-BC and the BCNC during isolation of BCNC step are presented in Figure 2a.

Table 1. Results of CrI calculation and thermal characteristics of the samples.

	Sample name				
	BC	DPBC	BCNC	PLA	PLA/BCNC-5%
CrI calculation (%)	60.7	73.6	79.6	23.8	42.7
Temperature (°C)					
T_g	105.0	105.0	105.0	61.4	61.4
T_m	113.8	348.7	282.8	154.2	152.7
T_d	160.7	381.3	318.6	–	–

From the diffraction intensity profiles shown that the peaks at 2θ = 14.6°, 16.8°, 22.6°, and 34.1°, are considered to 101, 10$\bar{1}$, 002 and 040 crystallographic planes,[35,36] and the rest ones are assigned to the amorphous contribution. The increases of amorphous content is the main contributor to peak broadening. The intrinsic factors that influence peak broadening are crystallite size and non-uniform strain within the crystal.[23] The presence of four crystallographic planes in all samples analyzed are characterized as cellulose crystal type Iα (triclinic), which are prevalent in BC, whereas the type Iβ crystal structure (monoclinic) was found in plant cellulose.[37] The Crystallinity for the three cellulose samples during isolation BCNC step were calculated and are shown in Table 1.

The CrI of the raw material native BC was 60.7% then increased after ultrasonic treatment (73.6%) and catalytic hydrolysis (79.6%). These results demonstrated that ultrasonic pretreatment can increase the crystallinity of cellulose, where the ultrasonic cavitation damaged the amorphous regions and the surface of crystalline regions leading to accelerate in hydrolysis of those areas. Therefore, it can be concluded that the ultrasonic pretreatment could improve these selectivity of catalytic hydrolysis. The possibility explanation may be likely that ultrasonic accelerates cellulose hydrolysis by creating localized erosion on the solid surface, thus increasing the reaction area and improving the accessibility of the catalyst metal chloride to the amorphous regions of cellulose. The degradation of amorphous regions during catalyzed hydrolysis can be explained by the Lewis acid character. According to Stein et al., 2010 [38], some metal chlorides such as $FeCl_3$, $AlCl_3$, $CuCl_2$, and $MnCl_2$ could form hydrated complexes in aqueous solution and coordinate the glycosidic oxygen of cellulose. This helps to scissor the glycosidic linkages and to facilitate the hydrolysis process, while the chloride anions attack the hydroxyl atoms.[39–41]

The effect of BCNC loading on the crystal structure of the biocomposites film (PLA/BCNC-5%w/w) is presented in Figure 2b. PLA is semicrystalline nature which shows a shoulder broadening curve from 11.5° to 18.1° that indicates as amorphous region. It also exhibits crystalline regions indicated by a prominent and sharp peak at 22.6° and 19.1° where the CrI was found about 23.8%. The incorporation of BCNC (5% w/w) into the matrix PLA led to increase in the intensity of the XRD peaks, which suggests an overall increase in the crystallinity of the biocomposites. However

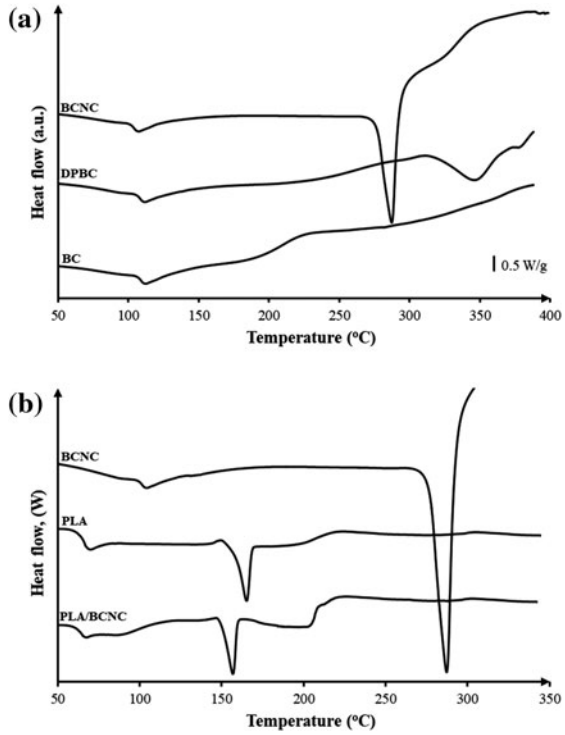

Figure 3. DSC thermograms of: (a) isolation of BCNC step (BC; D-BC; BCNC); (b) fabrication of biocomposite step (PLA; PLA/BCNC-5%).

this loading did not alter the diffraction patterns, which indicates that even although the crystallinity increased, there was no change in the crystal structure of PLA. The presence BCNC was noticeable by crystalline peaks at 16.8°, 22.6°, and 34.1°. The CrI of biocomposites were calculated and presented in Table 1 that was increase from 18.9%.

Thermal properties

DSC is a physical characterization method to study thermal behavior of basic polymers as well as the determination of their purity, stability and decomposition.[42–46] In general, cellulose thermal decomposition is complex simultaneous and consecutive chemical reactions which lead to cellulose pyrolysis and further combustion. Most of these reactions do not occur below 200 °C. However, all these thermal-physical changes and chemical reactions are highly dependent on the composition and physical nature of the cellulosic material, the ambient atmosphere, and the time of heating.[47] In this work, the glass transition temperature, T_g, crystalline melting point, T_m, and decomposition temperature, T_d were investigated to interpret thermal behaviors of the isolated samples. The thermograms for all cellulose samples: native BC, D-BC, and BCNC can be observed in Figure 3a.

The thermograms show that BC has different pattern from D-BC and BCNC. The heat-flow curve of all the samples displayed a small inflection of the baseline around 105.0 °C, which is the glass transition temperature, T_g, and is followed by an endothermic peak with the onset, T_m = 113.8 °C for the BC. For the samples D-BC and BCNC after the irradiation and hydrolysis treatment exhibit that the increased of CrI value, the endothermic peaks shifted toward a higher temperature. The endothermic curve of D-BC was distributed from 310 to 370 °C, with the crystalline melting temperature found at T_m = 348.7 °C. The peak was followed by a degradation temperature at T_d = 381.3 °C. A similar result was found for BCNC: an endothermic curve was found around 260-290 °C with the onset temperature at T_m = 282.8 °C then followed by degradation at T_d = 318.6 °C. The reason is that the thermal stability of nanocrystals is related to several factors including their dimension, crystallinity, and composition, which in turn depend on extraction conditions.[37,48] So, the BCNC with the highest crystallinity would exhibit the highest thermal stability, but smaller dimensions should also cause a decrease of the degradation temperature.

The effect of the loading BCNC (5% w/w) on the thermal properties of biocomposites PLA-BCNC are shown in Figure 3b. The corresponding data of the thermal beaviour are presented in Table 2. The figure indicates that the T_g of PLA was similar to that of the PLA/BCNC film. During the heating scan the T_g of PLA was observed to be 61.4 °C, while that of the nanocomposites remained constant around 61.0 °C This can be attributed to the lower interactions of the BCNC to change the mobility of polymer chains related to the glass transition.[49] The T_m of the biocomposites shows did not show a significant difference compared with that of the PLA. The melting peak of PLA is found at temperatures around 154.2 °C. The peak for PLA biocomposites containing BCNC is decreased slightly to the lower temperature at 152.8 °C with the broader shoulder around 200 °C as depicted in Figure 3b, indicating that overall the BCNC enhanced the crystallinity of the PLA biocomposites. Meanwhile the T_d of both samples, PLA and PLA/BCNC has the same temperature after 200 °C.

Surface morphology

The morphology of nanocrystals after the catalytic hydrolysis treatment was characterized by SEM observations. Figure 4a presents a SEM micrograph of sample BCNC. The sample was shown as fibrillated structure with variable length and smaller needles or nano-rods. It seems that the fibrillated structures are in fact constituted of the densely-packed needles. The BC-NC nano-rods are of (164.51 ± 7.56) nm in length with an average diameter of (25.05 ± 2.80) nm.

To observe the BCNC embedded in the PLA, representative SEM image of the morphology surface of the 5% (w/w) PLA/BCNC films is shown in Figure 4b. It can be seen that the matrix PLA was a relatively smooth surface but some aggregates were found which some agglomerated of BCNC were observed. However the biocomposite films had a good dispersion.

Mechanical properties

The mechanical properties were investigated to study for the effect of the loading of BCNC in the PLA biocomposites. The tensile strength and elongation at break are presented

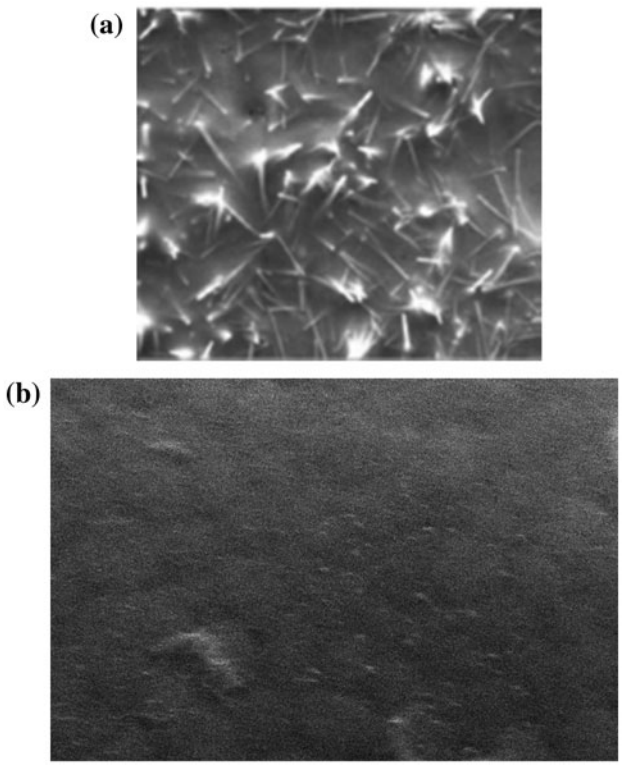

Figure 4. SEM — image of: (a) isolation of BCNC; (b) fabrication of biocomposite step (PLA; PLA/BCNC-5%).

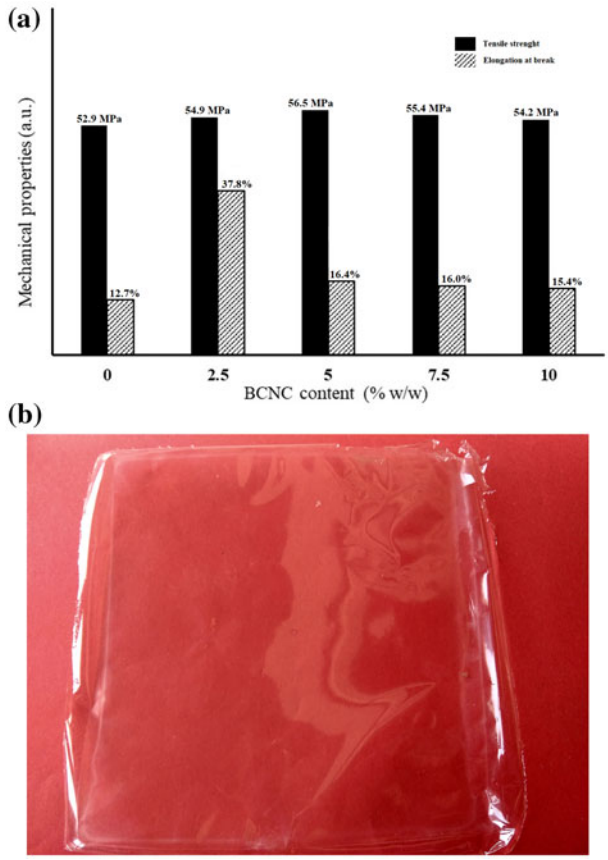

Figure 5. (a) Mechanical properties of the film PLA/BCNC bio-composites; (b) photographic image of bio-composite film containing 5% w/w of BCNC.

in Figure 5 show typical tensile stress-strain curves with different concentrations of the BCNC.

The mechanical properties and the appearance of the obtained film bio-composites are given in Figure 5. The tensile strength (TS) of the films (BCNC-0, BCNC-2.5, BCNC-5, BCNC-7.5, BCNC-10) are given in Figure 5a (black color). The results indicated that PLA films with various BCNC content showed more tensile strength than of pure PLA film (TS =52.9 MPa for sample BCNC-0). It is observed that tensile strength increases with increasing filler concentration, namely TS =54.9 MPa, 56.5 MPa, 55.4 MPa and 54.2 MPa MPa for sample BCNC-2.5, BCNC-5, BCNC-7.5 and BCNC-10 respectively. The increased tensile strength of the films with the increasing BCNC content indicated good dispersion of BCNC into PLA and strong interfacial actions between the PLA and BCNC. As expected the PLA-BCNC bio-composites exhibited enhanced tensile strength than pure PLA. The highest TS increased was observed about 3.6 MPa for the film containing 5% w/w of BCNC. This enhanced TS of PLA-BCNC bio-composites can be explained by the presence of crystalline content of BCNC. Elongation at break (Eb) of pure PLA film was found 12.7% (BCNC-0). For 2.5% w/w of BCNC (BCNC-2.5), 5% w/w (BCNC-5), 7.5% w/w (BCNC-7.5), 10% w/w (BCNC-10) film Eb were observed as 37.8%, 16.4%, 16.0%, and 15.4% respectively in Figure 5a (stripped color). The bio-composite films containing 5% w/w of BCNC in the matrix PLA yielded 56.5 MPa of tensile strength and Eb 16.4% of elongation at break indicated its high strength and low elongation. This results indicated a good indication that the material can be efficiently used as bone implants. The film, as can be seen from the photographic images, is transparent (Figure 5b). The preliminary result clearly indicates that the prepared BCNC could be used as a good reinforcing agent to prepare flexible transparent films

Conclusions

Bio-degradable film composites from PLA reinforced with BCNC were formulated by a solvent casting method and characterized. Needle and rod-like BCNC was successfully isolated from bacterial cellulose by catalytic hydrolysis using metal chloride salt ($FeCl_3.6H_2O$) assisted by ultrasonic irradiation and used as reinforcing agents. The mechanical properties bio-composites film were improved upon the incorporation of 5% w/w of BCNC into of PLA film, indicating that the material can be efficiently used as bone implants. The agglomeration of BCNC at higher concentrations could disturb the reinforcing effect on the tensile strength and elongation at break. Increased crystallinity of the PLA matrix was also observed by the nucleating effect of BCNC on the thermal properties. The BCNC isolated from bacterial cellulose can be used to overcome some drawbacks of biopolymer PLA film that limit its widespread application, with enhanced performance characteristics.

References

[1] Armentano, I.; Bitinis, N.; Fortunati, E.; Mattioli, S.; Rescignano, N.; Verdejo, R.; Lopez-Manchado, M. A.; Kenny,

J. M. Multifunctional Nanostructured PLA Materials for Packaging and Tissue Engineering. *Prog. Polym. Sci.* **2013**, *38*, 1720–1747. DOI: 10.1016/j.progpolymsci.2013.05.010.

[2] Rahmayetty, R.; Whulanza, Y.; Rahman, S.-F.; Suyono, E.-A.; Yohda, M.; Gozan, M. Use of Candida Rugosa Lipase as a Biocatalyst for L-Lactide Ring-Opening Polymerization and Polylactic Acid Production. *Biocatal. Agric. Biotechnol.* **2018**, *16*, 683–691. DOI: 10.1016/j.bcab.2018.09.015.

[3] Rasal, R.-M.; Janorkar, A.-V.; Hirt, D.-E. Poly (Lactic Acid) Modifications. *Prog. Polym. Sci.* **2010**, *35*, 338–356. DOI: 10.1016/j.progpolymsci.2009.12.003.

[4] Hiljanen-Vainio, H.; Varpomaa, P.; Seppälä, J.; Törmälä, P. Modification of Poly (l-Lactides) by Blending: mechanical and Hydrolytic Behavior. *Macromol. Chem. Phys.* **1996**, *197*, 1503–1523. DOI: 10.1002/macp.1996.021970427.

[5] Fortunati, E.; Aluigi, A.; Armentano, I.; Morena, F.; Emiliani, C.; Martino, S.; Santulli, C.; Torre, L.; Kenny, J.-M.; Puglia, D. Keratins Extracted from Merino Wool and Brown Alpaca Fibres: Thermal, Mechanical and Biological Properties of PLLA Based Biocomposites. *Mater. Sci. Eng. C.* **2015**, *47*, 394–406. DOI: 10.1016/j.msec.2014.11.007.

[6] Gui, Z.; Xu, Y.; Gao, Y.; Lu, C.; Cheng, S. Novel Polyethylene Glycol-Based Polyester-Toughened Polylactide. *Mater. Lett.* **2012**, *71*, 63–65. DOI: 10.1016/j.matlet.2011.12.045.

[7] Ramos, M.; Jiménez, A.; Peltzer, M.; Garrigós, M.-C. Development of Novel Nano-Biocomposite Antioxidant Films Based on Poly (Lactic Acid) and Thymol for Active Packaging. *Food Chem.* **2014**, *162*, 149–155. DOI: 10.1016/j.foodchem.2014.04.026.

[8] Peresin, M.-S.; Habibi, Y.; Zoppe, J.-O.; Pawlak, J.-J.; Rojas, O.-J. Nanofiber Composites of Polyvinyl Alcohol and Cellulose Nanocrystals: Manufacture and Characterization. *Biomacromolecules.* **2010**, *11*, 674–681. DOI: 10.1021/bm901254n.

[9] Zhang, W.; He, X.; Li, C.; Zhang, X.; Lu, C.; Zhang, X.; Deng, Y. High Performance Poly (Vinyl Alcohol)/Cellulose Nanocrystals Nanocomposites Manufactured by Injection Molding. *Cellulose.* **2014**, *21*, 485–494. DOI: 10.1007/s10570-013-0141-y.

[10] Abitbol, T.; Johnstone, T.; Quinn, T.-M.; Gray, D.-G. Reinforcement with Cellulose Nanocrystals of Poly (Vinyl Alcohol) Hydrogels Prepared by Cyclic Freezing and Thawing. *Soft Matter.* **2011**, *7*, 2373–2379. DOI: 10.1039/c0sm01172j.

[11] Siqueira, G.; Abdillahi, H.; Bras, J.; Dufresne, A. High Reinforcing Capability Cellulose Nanocrystals Extracted from Syngonanthus Nitens (Capim Dourado). *Cellulose.* **2010**, *17*, 289–298. DOI: 10.1007/s10570-009-9384-z.

[12] Bendahou, A.; Kaddami, H.; Dufresne, A. Investigation on the Effect of Cellulosic Nanoparticles' Morphology on the Properties of Natural Rubber Based Nanocomposites. *Eur. Polym. J.* **2010**, *46*, 629–620. DOI: 10.1016/j.eurpolymj.2009.12.025.

[13] Goffin, A.-L.; Raquez, J.-M.; Duquesne, E.; Siqueira, G.; Habibi, Y.; Dufresne, A.; Dubois, P.; Goffin, A.-L. Poly (ε-Caprolactone) Based Nanocomposites Reinforced by Surface-Grafted Cellulose Nanowhiskers via Extrusion Processing: morphology, Rheology, and Thermo-Mechanical Properties. *Polymer.* **2011**, *52*, 1532–1538. DOI: 10.1016/j.polymer.2011.02.004.

[14] Goffin, A.-L.; Raquez, J.-M.; Duquesne, E.; Siqueira, G.; Habibi, Y.; Dufresne, A.; Dubois, P. From Interfacial Ring-Opening Polymerization to Melt Processing of Cellulose Nanowhisker-Filled Polylactide-Based Nanocomposites. *Biomacromolecules.* **2011**, *12*, 2456–2465. DOI: 10.1021/bm200581h.

[15] Raquez, J.-M.; Murena, Y.; Goffin, A.-L.; Habibi, Y.; Ruelle, B.; DeBuyl, F.; Dubois, P. Surface-Modification of Cellulose Nanowhiskers and Their Use as Nanoreinforcers into Polylactide: A Sustainably-Integrated Approach. *Compos. Sci. Technol.* **2012**, *72*, 544–549. DOI: 10.1016/j.compscitech.2011.11.017.

[16] Siqueira, G.; Bras, J.; Follain, N.; Belbekhouche, S.; Marais, S.; Dufresne, A. Thermal and Mechanical Properties of Bio-Nanocomposites Reinforced by Luffa Cylindrica Cellulose Nanocrystals. *Carbohydr. Polym.* **2013**, *91*, 711–717. DOI: 10.1016/j.carbpol.2012.08.057.

[17] Rahmayetty, S.,B.; Prasetya, G.,M. Synthesis and characterization of L-lactide and polylactic acid (PLA) from L-lactic acid for biomedical applications. In AIP Conference Proceedings, **2017**, 1817, 020009. DOI: 10.1063/1.4976761.

[18] Wardhono, E.-Y.; Wahyudi, H.; Agustina, S.; Oudet, F.; Pinem, M.-P.; Clausse, D.; Saleh, K.; Guénin, E. Ultrasonic Irradiation Coupled with Microwave Treatment for Eco-Friendly Process of Isolating Bacterial Cellulose Nanocrystals. *Nanomaterials.* **2018**, *859*, 2018. DOI: 10.3390/nano8100859.

[19] George, J.; Ramana, K.-V.; Bawa, A.-S. Bacterial Cellulose Nanocrystals Exhibiting High Thermal Stability and Their Polymer Nanocomposites. *Int. J. Biol. Macromol.* **2011**, *48*, 50–57. DOI: 10.1016/j.ijbiomac.2010.09.013.

[20] Azizi Samir, M.-A.-S.; Alloin, F.; Dufresne, A. Review of Recent Research into Cellulosic Whiskers, Their Properties and Their Application in Nanocomposite Field. *Biomacromolecules.* **2005**, *6*, 612–626. DOI: 10.1021/bm0493685.

[21] Vieira, M.-G.-A.; Da Silva, M.-A.; Dos Santos, L.-O.; Beppu, M.-M. Natural-Based Plasticizers and Biopolymer Films: A Review. *Eur. Polym. J.* **2011**, *47*, 254–263. DOI: 10.1016/j.eurpolymj.2010.12.011.

[22] Wardhono, E.-Y.; Kanani, N.; Alfirano, A. A Simple Process of Isolation Microcrystalline Cellulose Using Ultrasonic Irradiation. *J. Dispers. Sci. Technol.* **2019**, 1. DOI: 10.1080/01932691.2019.1614947.

[23] Park, S.; Baker, J.-O.; Himmel, M.-E.; Parilla, P.-A.; Johnson, D.-K. Cellulose Crystallinity Index: measurement Techniques and Their Impact on Interpreting Cellulase Performance. *Biotechnol. Biofuels.* **2010**, *3*, 10–21. doi.org/10.1186/1754-6834-3-10. DOI: 10.1186/1754-6834-3-10.

[24] Kruer-Zerhusen, N.; Cantero-Tubilla, B.; Wilson, D.-B. Characterization of Cellulose Crystallinity after Enzymatic Treatment Using Fourier Transform Infrared Spectroscopy (FTIR). *Cellulose.* **2018**, *25*, 37–48. DOI: 10.1007/s10570-017-1542-0.

[25] Kondo, T. The Assignment of IR Absorption Bands Due to Free Hydroxyl Groups in Cellulose. *Cellulose.* **1997**, *4*, 281–290. DOI: 10.1023/A:1018448109214.

[26] Börjesson, M.; Crystalline, W.,G. nanocellulose—preparation, modification, and properties. In *Cellulose-Fundamental Aspects and Current Trends*, InTech, **2015**.

[27] Chang, W.-S.; Chen, H.-H. Physical Properties of Bacterial Cellulose Composites for Wound Dressings. *Food Hydrocoll.* **2016**, *53*, 75–83. DOI: 10.1016/j.foodhyd.2014.12.009.

[28] Ornaghi, H.-L.; Poletto, H.; Zattera, A.-J.; Amico, S.-C. Correlation of the Thermal Stability and the Decomposition Kinetics of Six Different Vegetal Fibers. *Cellulose.* **2014**, *21*, 177–188. DOI: 10.1007/s10570-013-0094-1.

[29] AAkerholm, M.; Hinterstoisser, B.; Salmén, L. Characterization of the Crystalline Structure of Cellulose Using Static and Dynamic FT-IR Spectroscopy. *Carbohydr. Res.* **2004**, *339*, 569–578. DOI: 10.1016/j.carres.2003.11.012.

[30] Xu, J.; Zhang, J.; Gao, W.; Liang, H.; Wang, H.; Li, J. Preparation of Chitosan/PLA Blend Micro/Nanofibers by Electrospinning. *Mater. Lett.* **2009**, *63*, 658–660. DOI: 10.1016/j.matlet.2008.12.014.

[31] Zhou, Z.-F.; Huang, G.-Q.; Xu, W.-B.; Ren, F.-M. Chain Extension and Branching of Poly (L-Lactic Acid) Produced by Reaction with a DGEBA-Based Epoxy Resin. *Express Polym. Lett.* **2007**, *1*, 734–739. DOI: 10.3144/expresspolymlett.2007.101.

[32] Dhar, P.; Tarafder, D.; Kumar, A.; Katiyar, V. Effect of Cellulose Nanocrystal Polymorphs on Mechanical, Barrier and Thermal Properties of Poly (Lactic Acid) Based Bionanocomposites. *RSC Adv.* **2015**, *5*, 60426–60440. DOI: 10.1039/C5RA06840A.

[33] Hult, E.-L.; Iversen, T.; Sugiyama, J. Characterization of the Supermolecular Structure of Cellulose in Wood Pulp Fibres. *Cellulose.* **2003**, *10*, 103–110. DOI: 10.1023/A:1024080700873.

[34] Garvey, C.-J.; Parker, I.-H.; Simon, G.-P. On the Interpretation of X-Ray Diffraction Powder Patterns in Terms of the Nanostructure of Cellulose I Fibres. *Macromol. Chem. Phys.* **2005**, *206*, 1568–1575. DOI: 10.1002/macp.200500008.

[35] He, J.; Cui, S.; Wang, S. Preparation and Crystalline Analysis of High-Grade Bamboo Dissolving Pulp for Cellulose Acetate. *J. Appl. Polym. Sci.* **2008**, *107*, 1029–1038. DOI: 10.1002/app.27061.

[36] Nishiyama, Y.; Sugiyama, J.; Chanzy, H.; Langan, P. Crystal Structure and Hydrogen Bonding System in Cellulose Iα from Synchrotron X-Ray and Neutron Fiber Diffraction. *J. Am. Chem. Soc.* **2003**, *125*, 14300–14306. DOI: 10.1021/ja037055w.

[37] Henrique, M.-A.; Neto, W.-P.-F.; Silvério, H.-A.; Martins, D.-F.; Gurgel, L.-V.-A.; Barud, H. S.; Morais, L.-C.; Pasquini, D. Kinetic Study of the Thermal Decomposition of Cellulose Nanocrystals with Different Polymorphs, Cellulose I and II, Extracted from Different Sources and Using Different Types of Acids. *Ind. Crops Prod.* **2015**, *76*, 128–140. DOI: 10.1016/j.indcrop.2015.06.048.

[38] Stein, T.-V.; Grande, P.; Sibill, F.; Commandeur, U.; Fischer, R.; Leitner, W.; María, P.-D. Salt-Assisted Organic-Acid-Catalyzed Depolymerization of Cellulose. *Green Chem.* **2010**, *12*, 1844–1849. DOI: 10.1039/c0gc00262c.

[39] Kamireddy, S.-R.; Li, J.; Tucker, M.; Degenstein, J.; Ji, Y. Effects and Mechanism of Metal Chloride Salts on Pretreatment and Enzymatic Digestibility of Corn Stover. *Ind. Eng. Chem. Res.* **2013**, *52*, 1775–1782. DOI: 10.1021/ie3019609.

[40] Lu, Q.; Tang, L.; Lin, F.; Wang, S.; Chen, Y.; Chen, X.; Huang, B. Preparation and Characterization of Cellulose Nanocrystals via Ultrasonication-Assisted FeCl 3-Catalyzed Hydrolysis. *Cellulose* **2014**, *21*, 3497–3506. DOI: 10.1007/s10570-014-0376-2.

[41] Ma, Y.; Ji, W.; Zhu, X.; Tian, L.; Wan, X. Effect of Extremely Low AlCl3 on Hydrolysis of Cellulose in High Temperature Liquid Water. *Biomass Bioenergy.* **2012**, *39*, 106–111. DOI: 10.1016/j.biombioe.2011.12.033.

[42] Clausse, D.; Wardhono, E.-Y.; Lanoiselle, J.-L. Formation and Determination of the Amount of Ice Formed in Water Dispersed in Various Materials. *Colloids Surf. Physicochem. Eng. Asp.* **2014**, *460*, 519–526. DOI: 10.1016/j.colsurfa.2014.06.032.

[43] Zafimahova-Ratisbonne, A.; Wardhono, E.-Y.; Lanoisellé, J.-L.; Saleh, K.; Clausse, D. Stability of W/O Emulsions Encapsulating Polysaccharides. *J. Dispers. Sci. Technol* **2014**, *35*, 38–47. DOI: 10.1080/01932691.2013.773444.

[44] Wardhono, E.-Y.; Zafimahova-Ratisbonne, A.; Lanoiselle, J.-L.; Saleh, K.; Clausse, D. Optimization of the Formulation of Water in Oil Emulsions Entrapping Polysaccharide by Increasing the Amount of Water and the Stability. *Can. J. Chem. Eng.* **2014**, *92*, 1189–1196. DOI: 10.1002/cjce.21985.

[45] Wardhono, E.-Y.; Zafimahova-Ratisbonne, A.; Saleh, K.; Clausse, D.; Lanoiselle, J.-L. W/O Emulsion Destabilization and Release of a Polysaccharide Entrapped in the Droplets. *J. Dispers. Sci. Technol.* **2016**, *37*, 1581–1589. DOI: 10.1080/01932691.2015.1118704.

[46] Gregorova, A. Application of differential scanning calorimetry to the characterization of biopolymers. in *Applications of Calorimetry in a Wide Context-Differential Scanning Calorimetry, Isothermal Titration Calorimetry and Microcalorimetry*, InTech, **2013**.

[47] Bertran, M.-S.; Dale, B.-E. Determination of Cellulose Accessibility by Differential Scanning Calorimetry. *J. Appl. Polym. Sci.* **1986**, *32*, 4241–4253. DOI: 10.1002/app.1986.070320335.

[48] Jonoobi, M.; Oladi, R.; Davoudpour, Y.; Oksman, K.; Dufresne, A.; Hamzeh, Y.; Davoodi, R. Different Preparation Methods and Properties of Nanostructured Cellulose from Various Natural Resources and Residues: A Review. *Cellulose.* **2015**, *22*, 935–969. DOI: 10.1007/s10570-015-0551-0.

[49] Fortunati, E.; Luzi, F.; Puglia, D.; Dominici, F.; Santulli, C.; Kenny, J.-M.; Torre, L. Investigation of Thermo-Mechanical, Chemical and Degradative Properties of PLA-Limonene Films Reinforced with Cellulose Nanocrystals Extracted from Phormium Tenax Leaves. *Eur. Polym. J.* **2014**, *56*, 7–91. DOI: 10.1016/j.eurpolymj.2014.03.030.